Modelling and Synchronization of Pulse-Coupled Non-identical Oscillators for Wireless Sensor Networks

Yan Zong, Xuewu Dai, Zhiwei Gao, Krishna Busawon, Jiwen Zhu
Department of Mathematics, Physics and Electrical Engineering
Northumbria University
Newcastle upon Tyne, United Kingdom
{yan.zong, xuewu.dai, zhiwei.gao, krishna.busawon, jiwen.zhu}@northumbria.ac.uk

***Abstract*—Time synchronization in wireless sensor networks, aiming to provide a common sense of timing among distributed sensor nodes, is a key enabling technology for many applications, such as collaborative condition monitoring, time-of-flight localization and underwater navigation and tactical surveillance. In order to solve the challenges of the manufacturing tolerance and working condition variations in any real-world environments, a novel state-space model for pulse-coupled non-identical oscillators is proposed to model a realistic clock oscillator with non-identical and time-varying frequency. A state feedback correction, referred to as hybrid coupling mechanism, is also proposed to ensure the system move into steady state, thus achieving time synchronization in wireless sensor networks. Furthermore, the intensive simulations of single-hop wireless sensor networks have been carried out to evaluate the performance of proposed pulse-coupled non-identical oscillators. It is shown that a partially-connected wireless network consisting of 50 non-identical pulse-coupled oscillators can achieve the synchronization with the precision of $40us$.**

***Index Terms*—time synchronization, pulse-coupled oscillators, hybrid coupling, proportional controller, wireless sensor networks**

I. Introduction

Time Synchronization (TS) in Wireless Sensor Networks (WSNs), aiming to provide a common sense of timing among distributed sensor nodes, is a key enabling technology for many WSNs applications, such as collaborative condition monitoring, coordinated control, time-of-flight localization and underwater navigation and tactical surveillance. In such applications, a network of distributed sensors is dedicated to cooperatively monitor physical or environmental conditions such as location, sound and pressure at different locations, which requires precise timing among sensor nodes.

As common WSN embedded systems, the clock of a sensor node is usually generated using a crystal oscillator. Evidently, as one would expect, the clocks of these sensor nodes are not necessarily identical due to the manufacturing tolerance. More precisely, the frequency and the phase of the clocks might be different from each other. Additionally, a clock drift might also occur due to working condition variations, such as power supply voltage and temperature. The purpose of time synchronization is to make the phase and frequency of the non-identical sensor node clocks converge to the phase and frequency of the *reference clock* so that, eventually, all the clocks in a sensor network will have the same phase and frequency once the synchronization is achieved.

Mathematically speaking, the target of the time synchronization is to keep the sensor nodes clocks phase differences and frequency differences with respective to the *reference clock* as small as possible. In the computer science community, time synchronization is achieved by periodically exchanging timestamped packet among paired nodes to acquire the time difference of two clocks. Once the time difference is measured through the packet exchange communication protocol, a sensor node adjusts its clocks phase and frequency accordingly to approach the *reference time*.

Owing to its foundation and significance, time synchronization has attracted a lot of attention in mathematics and physics community. It is also investigated under the topic of networked oscillators, consisting of a set of oscillators whose phases are pair-wise coupled. A typical model of networked oscillators is the well-known Pulse-Coupled Oscillators (PCO) that is inspired by fireflies behavior and Peskin's model for self-synchronization of cardiac pacemaker. It is important to note that most theoretical work dealing with phase-coupling, which is the procedure of exchanging phase values among oscillators by comparing their phase difference and compensating its phase and frequency to achieve a common value, is carried out in continuous-time domain. On the other hand, the phase-coupling (also named with pulse-coupling) in PCO is episodic and pulse-like [11].

A. Related Work

In the classical PCO, an oscillator works either in free-running mode or interactive mode. In the free-running mode, the oscillator behaves as an standalone uncoupled oscillator. Its clock state, which is denoted by P, rises toward threshold value. When P reaches the threshold, the oscillator fires, a *Pulse* is generated and clock state is reset, after which the cycle repeats.

In the interactive mode, in addition to the clock state evolves as mentioned in the free-running mode, the clock

978-1-5386-4829-2/18/$31.00 ©2018 IEEE

state P is pulled up by one constant coupling strength (i.e., excitatory coupling), upon the reception of a *Pulse* from another node. The inhibitory coupling, where P is pulled down when receipting a *Pulse*, can also be used in the interactive mode. However, PCO can only adopt excitatory coupling or inhibitory coupling in interactive mode.

Packet-exchange time synchronization in WSNs can be modelled as pulse-coupled oscillators, where the periodical packet transmission is equivalent to *Pulse* firing. From the viewpoint of PCO, the clocks in wireless sensor nodes are equivalent to oscillators in PCO. It is well known that, clock in embedded systems is implemented by a *counter* driving by a crystal oscillator. The *counter* is reset when its value reaches a predefined threshold. This indeed is similar to the firing-resetting procedure of PCO, where the oscillator fires and its state is reset to zero periodically. Thus, the term *oscillator* will be used when describing the mathematical model, and the term (*wireless sensor*) *node* is adopted when describing the model implementation in the wireless sensor networks.

PCO has attracted a lot of attention over years due to its inherent scalability and simplicity, which are beneficial to large-scale distributed wireless networks applications with low energy cost [13]. However, some limitations of classical PCO by Mirollo and Strogatz restricting application to the realistic WSNs stem from following assumptions: (i) identical internal dynamics of oscillators (i.e., the frequency of all oscillators is same), (ii) ideal pulse-coupling (i.e., oscillators actual phases are instantly known to its neighboring oscillators and zero delay between coupled oscillators), (iii) fully-connected network topology (i.e., all-to-all coupling strategy). All of the aforementioned assumptions are not true when it comes to any real-world environments, and the classical PCO needs to be improved in order to be implemented in realistic networks. This paper focuses on the problem of non-identical oscillators.

Over the years, many PCO clock models have been proposed for synchronization of WSNs. These can be divided into three categories: (i) identical and constant oscillator frequency, (ii) non-identical however constant frequency of oscillators, (iii) non-identical and time-varying frequency of oscillators.

In effect, in [11] the synchronization of the PCO model with excitatory coupling and constant and identical frequency among a large population of oscillators was proposed and proved. In [1] it was proved that the instantaneous synchronization of the PCO with excitatory coupling and the different frequency (i.e., the frequency of oscillators is constant, but nevertheless, non-identical) can be achieved under some specified conditions. By using the inhibitory coupling mechanism, [10] simulated a system of 10 pulse-coupled oscillators with small difference in frequencies can obtain the synchronization with the precision bounded by the upper bound. Moreover, it is also shown that inhibitory coupling can attain the same precision as excitatory coupling [10].

However, due to the manufacturing tolerance and working condition variations, the oscillator frequency is non-identical and time-varying, and the assumption of identical oscillators cannot be met in practice. For example, the frequency drift ranges from ± 5 Parts Per Million (PPM) to ± 100PPM depending on the quality of the crystal oscillators [3], [14], [15]. Even though [2] achieve the synchronization by implementing PCO into the heterogeneous system (i.e., realistic wireless sensor nodes with non-identical and time-varying oscillator frequency), to the best knowledge of the authors, it still lacks non-identical and time-varying PCO mathematical clock model and the proofs of achieving the synchronization.

B. Contribution and Paper Organization

To derive an accurate model for a realistic PCO clock (i.e., non-identical and time-varying PCO mathematical clock), the behavior of clock is modelled using the state-space approach. This approach is considered in several works (e.g., [7] and [9]), and has the advantage that specific features of clock behavior can be described as well as leading to the consideration of a proportional controller in the implementation of PCO interactive mode.

The classical clock correction method, excitatory coupling, is adopted among many literatures (e.g., [1], [11]). Inhibitory coupling is also analyzed and simulated in [5], [10]. However, in those literatures, PCO can only adopt excitatory coupling or inhibitory coupling. In this work, a hybrid coupling mechanism, combing excitatory coupling and inhibitory coupling, is proposed to correct the drifting clock based on the reception of *Pulse*. In the hybrid coupling mechanism, rather than correcting the clock state by constant coupling strength, the offset between coupled oscillators is calculated to correct the drifting clock by using the local timestamp.

In this paper, a novel state-space model for the non-identical and time-varying PCO is proposed. Next, a state feedback clock correction, namely, the hybrid coupling mechanism, is proposed and presented to enable the closed-loop system to converge to the steady state (i.e., time synchronization is achieved in WSNs). Moreover, two scenarios of network topologies are simulated to evaluate the performance of proposed hybrid coupling mechanism.

The rest of this paper is as follows: the proposed PCO clock model with non-identical and time-varying frequency is first derived in Section 2. Next, in Section 3 the timestamp which is generated on local clock time based on the reception of received *Pulse* is introduced. The hybrid coupling mechanism (i.e., state feedback clock correction), to correct the drifting PCO clock is presented in Section 4. Simulation results are given in Section 5. Finally, conclusion is drawn in Section 6.

II. State-Space Model of Non-identical Oscillator Clock

This paper considers a cluster of single-hop wireless sensor nodes consisting of one cluster-head node and a set of sensor nodes, as illustrated in Fig. 1. A sensor node in the cluster networks can communicate with at least one neighboring node. The cluster-head node can communicate with all sensor nodes in single-hop, and is equipped with a Global Positioning System (GPS) clock to provide *reference clock* to all sensor nodes. This clock is referred to as master clock thereafter

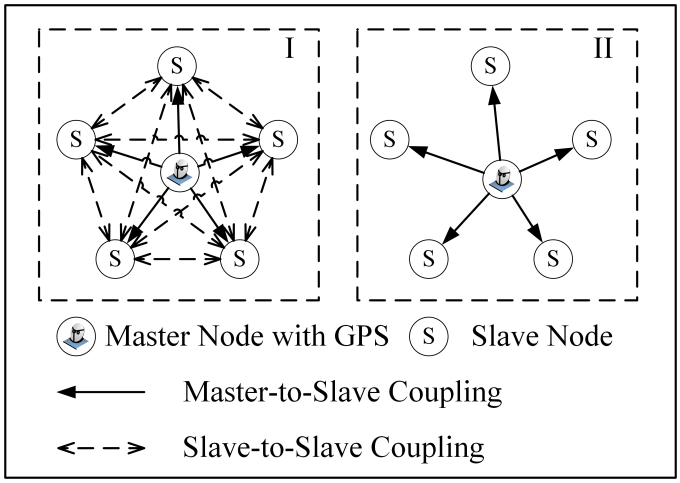

Fig. 1. Network Topology (I: Fully-Connected Wireless Sensor Network, II: Partially-Connected Wireless Sensor Network).

in this paper, and the cluster-head node and sensor node are called master node and slave node respectively.

It is worth noting that, the PCO model of time synchronization in such a practical wireless sensor network is different from the classical PCO in two aspects: (i) a master oscillator presents and works as a pacemaker, (ii) the slave oscillators are non-identical. The master node's clock can be regarded as a perfect oscillator running exactly at its nominal frequency with zero initial phase. The sensor node's clocks can be regarded as drifting non-identical oscillators with non-identical nominal frequencies and different initial phase.

As illustrated in Fig. 1, this paper considers two scenarios of network topologies. The first one is a fully-connected network, where a sensor node can communicate with each node in the network. Such a topology meets the classical PCO's assumption of full connectivity. However, full connection is a restrictive requirement, which is difficult to achieve in practice due to partial connections caused by constraints of transmission power and Radio Frequency (RF) module's sensitivity. A typical phenomenon of partial connectivity in WSNs is the well-known problem of hidden terminal. Take this into account, Fig. 1.(II) illustrates the second network topology considered in this paper, where each sensor node only communicates with the cluster-head node for synchronization.

As a digital system, the clock of an embedded system is a discrete clock driven by a crystal oscillator through a *counter*. Assume a crystal oscillator runs at its nominal frequency f_0 and the discrete clock is updated periodically at an interval $\tau_0 = 1/f_0$. Let $t[n]$ denote the actual time at the n-th clock update event, $t[n]$ is also known as the *reference time*, let $C[n]$ represent the clock time of a node at the n-th clock update event. For a perfect clock, such as the GPS clock at the cluster-head node, $C[n] = t[n] = n\tau_0$. At a sensor node, a drifting clock can be described as [16]

$$C[n] = t[n] + \frac{\sum_{n=0}^{n-1}\alpha[n]\tau_0}{f_0} + \phi[n] \tag{1}$$

where $\alpha[n]$ denotes the frequency deviation of the drifting oscillator at time $t[n]$ and the actual frequency $f[n]$ of a drifting clock is (f_0+$\alpha[n]$). In addition, $\phi[n]$ is the instant phase noise, which can be modelled as a random process.

In PCO model, a clock is represented by a state variable P that increases linearly from zero to threshold value defined by φ. Once P reaches the threshold φ, P is reset to 0, after which a *Pulse* is immediately fired and broadcasted to other oscillators for synchronization. Similarly, in WSNs, the threshold of a *counter* can be set to the same value of φ to have the same time synchronization cycle. Since the clock threshold φ is greater than the clock update interval τ_0 (i.e., $\varphi \gg \tau_0$), assuming the clock is updated m time during one synchronization cycle yields $\varphi = m\tau_0$.

Taking the periodical resetting behavior of PCO into account, at the n-th clock update event, the drifting PCO clock's state $P[n]$ can be modelled by comparing classic drifting clock $C[n]$ against sum of threshold ($\sum_{n=1}^{\lfloor \frac{n}{m} \rfloor}\varphi[n]$). That is

$$\begin{aligned} P[n] &= C[n] - \sum_{n=1}^{\lfloor \frac{n}{m} \rfloor}\varphi[n] \\ &= t[n] + \frac{\sum_{n=0}^{n-1}\alpha[n]\tau_0}{f_0} + \phi[n] - \sum_{n=1}^{\lfloor \frac{n}{m} \rfloor}\varphi[n] \end{aligned} \tag{2}$$

where the floor operator $\lfloor x \rfloor$ means the largest integer not greater than x.

Clock offset is the difference between the drifting clock $C[n]$ and the *reference clock* $t[n]$. To obtain a more succinct PCO clock state-space model, it can be seen from (2) that the clock offset $\theta[n]$ of a PCO in the embedded systems is the accumulated phase deviation caused by drifting frequency $\frac{\sum_{n=0}^{n-1}\alpha[n]\tau_0}{f_0}$, phase noise $\phi[n]$ minus the sum of threshold $\sum_{n=1}^{\lfloor \frac{n}{m} \rfloor}\varphi[n]$.

$$\theta[n] = \frac{\sum_{n=0}^{n-1}\alpha[n]\tau_0}{f_0} + \phi[n] - \sum_{n=1}^{\lfloor \frac{n}{m} \rfloor}\varphi[n] \tag{3}$$

As usual, drifting frequency of non-identical PCO is characterized by clock skew $\gamma[t[n]] = \frac{f[t[n]]-f_0}{f_0}$. It is a dimensionless quantity denoting the deviation of frequency from the nominal frequency f_0. In the discretized clock model, $\gamma[n] = \frac{\alpha[n]}{\tau_0}$ is for one clock update interval of $[t[n],\ t[n+1]]$. Therefore, by introducing $\bar{\omega}_\theta[n] = \phi[n+1] - \phi[n]$, the offset at the $(n+1)$-th clock update event can be expressed in an iterative form as

$$\theta[n+1] = \begin{cases} \theta[n] + \gamma[n]\tau_0 + \bar{\omega}_\theta[n], & if\ \frac{n}{m} \notin Z \\ \theta[n] + \gamma[n]\tau_0 + \bar{\omega}_\theta[n] - \varphi, & if\ \frac{n}{m} \in Z \end{cases} \tag{4}$$

where Z represents the set of positive integers $\{1, 2, 3...\}$ and $\frac{n}{m} \in Z$ indicates the occurrence of PCO clock's state resetting and *Pulse* firing.

[8] introduces an improved clock skew model, first-order auto-regressive (AR) model, by considering the phase noise

of oscillator and clock skew with certain randomness that is not completely independent for each sample. According to the assumption that the skew $\gamma[n]$ is of slow change as well, the skew of the $(n+1)$-th event, described as a time-varying process in an auto-regressive manner with a small perturbation, is defined as

$$\gamma[n+1] = p\gamma[n] + \bar{\omega}_\gamma[n] \tag{5}$$

where p, denoting the parameter of the first-order AR model, is a positive number less than but close to 1, and $\bar{\omega}_\gamma$ indicates the model noise with zero mean. In addition, both offset noise $\bar{\omega}_\theta$ and skew noise $\bar{\omega}_\gamma$, two uncorrelated random process, are subjected to zero-mean gaussian distribution with standard deviation σ_θ and σ_γ respectively [16].

Equation (4) and (5), describing the drifting PCO clock, can be rewritten in matrix form

$$\begin{aligned}
\begin{bmatrix} \theta[n+1] \\ \gamma[n+1] \end{bmatrix} &= \begin{bmatrix} 1 & \tau_0 \\ 0 & p \end{bmatrix} \begin{bmatrix} \theta[n] \\ \gamma[n] \end{bmatrix} + \begin{bmatrix} 0 \\ 0 \end{bmatrix} [\varphi] \\
&\quad + \begin{bmatrix} \bar{\omega}_\theta[n] \\ \bar{\omega}_\gamma[n] \end{bmatrix}, if \frac{n}{m} \notin Z \\
\begin{bmatrix} \theta[n+1] \\ \gamma[n+1] \end{bmatrix} &= \begin{bmatrix} 1 & \tau_0 \\ 0 & p \end{bmatrix} \begin{bmatrix} \theta[n] \\ \gamma[n] \end{bmatrix} + \begin{bmatrix} -1 \\ 0 \end{bmatrix} [\varphi] \\
&\quad + \begin{bmatrix} \bar{\omega}_\theta[n] \\ \bar{\omega}_\gamma[n] \end{bmatrix}, if \frac{n}{m} \in Z
\end{aligned} \tag{6}$$

By defining the PCO clock state vector $x[n] = [\theta[n], \gamma[n]]^T$, PCO clock input matrix $\mu[n] = [\varphi]$, and process noise matrix $\bar{\omega}[n] = [\bar{\omega}_\theta[n], \bar{\omega}_\gamma[n]]^T$, the PCO clock state-space model at the l-th time synchronization cycle is described as

$$x[lm+m] = A^m x[lm] + G\mu[lm] + L\Omega[lm] \tag{7}$$

where $A = \begin{bmatrix} 1 & \tau_0 \\ 0 & p \end{bmatrix}$ represents the PCO clock state transition matrix, $G = \begin{bmatrix} -1 \\ 0 \end{bmatrix}$ denotes PCO clock input transition matrix, $L = \left[A^{m-1}, A^{m-2}, ..., A, E\right]^T$ is the time synchronization transition matrix, and $\Omega[lm] = [\bar{\omega}[lm], \bar{\omega}[lm+1], ..., \bar{\omega}[(l+1)m-2], \bar{\omega}[(l+1)m-1]]$ means the time synchronization noise matrix. To simplify the analysis, the (7) is simplified to

$$x[k+1] = A^m x[k] + G\mu[k] + \omega[k] \tag{8}$$

where $\omega[k] = L\Omega[lm]$ represents the PCO clock state noise matrix, and (8) is to denote the PCO state-space model at the k-th time synchronization cycle (i.e., the l-th time synchronization cycle).

It is worth noting that the proposed clock model of (8) can represent both perfect non-drifting clock and drifting PCO clock. If both clock offset and skew are zero (i.e., $\theta[k] = 0$, $\gamma[k] = 0$, $\omega_\theta[k] = 0$ and $\omega_\gamma[k] = 0$), the clock of (8) is perfect clock without frequency drifting. Otherwise, (8) is to generate the drifting PCO clock time information.

III. Timestamped Packet Exchange And Pulse Coupling

In the embedded systems, the physical waveform (i.e., *Pulse*) of PCO cannot be generated and broadcasted, however, the packet named with *SYNC* can be adopted to model the PCO *Pulse*. The proposed clock measurement algorithm provides means for estimating the offset and drift of a local drifting clock through the reception of *SYNC* packet containing timestamp generated by the local clock. Specifically, during the k-th time synchronization cycle, both node i and j fire and broadcast the *SYNC* packet. On the reception of *SYNC* of node j, the node i associates a timestamp $\hat{P}_{ij}[k]$ from the local time to the received *SYNC*.

Using the local timestamp, the node i can directly determine its measurement offset at the k-th synchronization cycle

$$\hat{\theta}_{ij}[k] = \begin{cases} \hat{P}_{ij}[k] - \kappa & if \quad \hat{P}_{ij}[k] < \frac{\varphi_i[k]}{2} \\ \hat{P}_{ij}[k] - \kappa - \varphi_i[k] & if \quad \hat{P}_{ij}[k] \geq \frac{\varphi_i[k]}{2} \end{cases} \tag{9}$$

where $\hat{\theta}_{ij}[k]$ denotes the measurement offset of node i based on the reception of *SYNC* from the j-th node. $\varphi_i[k]$ is the PCO clock state threshold of node i at the k-th time synchronization cycle. κ represents the transmission delay of *SYNC* packet to transmit/receipt to/from the wireless channel. The variable $\hat{\theta}[k]$ is used to represent $\hat{\theta}_{ij}[k]$ to simplify the analysis.

Owning to the hybrid coupling mechanism, the measurement clock offset $\hat{\theta}[k-1]$ is corrected at the $(k-1)$-th time synchronization cycle. By assuming the measurement offset is constant in a time synchronization cycle, the measurement skew $\hat{\gamma}[k]$ therefore is

$$\hat{\gamma}[k] = \frac{\hat{\theta}[k]}{\varphi} \tag{10}$$

It is notable that, in the embedded systems, timestamp is usually implemented by software, either in an interrupt or a polling scheme. *Software timestamp* will not only introduce delays into the timestamp but also the uncertainties caused by the packet transmission between the *physical layer* and the upper layer. The measurement offset and skew are therefore affected by timestamping uncertainties ΔP of the local clock. For the purposes of analysis, timestamping uncertainties are denoted by random variables with finite standard deviation σ_η whose values can be varied to consider different timestamping performances [7]. The ideal timestamp $P[k]$ at the k-th time synchronization cycle is

$$P[k] = \hat{P}[k] - \Delta P[k] \tag{11}$$

By defining the measurement offset uncertainties $\nu_\theta[k] = \Delta P[k]$ with standard deviation σ_η, and let $\nu_\gamma[k] = \Delta\gamma[k]$ denote the skew model error, which is subject to the zero-mean gaussian distribution noise. The uncertainties associated to the measurement (9), (10) can be described as

$$\begin{cases} \hat{\theta}[k] = \theta[k] + \nu_\theta[k] \\ \hat{\gamma}[k] = \gamma[k] + \nu_\gamma[k] \end{cases} \tag{12}$$

The above clock offset and skew measurement procedure can be interpreted as a soft sensor for offset and skew measurement. From the point of view of state-space, the procedure forms the observation equation

$$y[k] = Cx[k] + \nu[k] \tag{13}$$

where $C = \begin{bmatrix} 1 & 0 \\ 0 & 1 \end{bmatrix}$ is the observation matrix of PCO that maps the PCO clock state vector into the measurement domain, and $\nu[k] = \begin{bmatrix} \nu_\theta[k] \\ \nu_\gamma[k] \end{bmatrix}$ is the matrix of measurement uncertainties.

IV. State Feedback Clock Correction

This paper adopts the attenuated correction method (i.e., proportional controller) to correct the clock offset and skew of the drifting PCO clock via applying the partially measured offset and skew, and the correction scheme can be modelled mathematically by

$$\begin{cases} \theta[k+1] = \theta[k] + u_\theta[k] \\ \gamma[k+1] = \gamma[k] + u_\gamma[k] \end{cases} \tag{14}$$

Specifically, in Fig. 2, the set point matrix is configured to $[0,0]^T$ to ensure the offset and skew of drifting PCO clock convergence to zero after infinite time synchronization cycles (i.e., $k \to +\infty$), namely, time synchronization of network is achieved. The error signal $e[k]$, defined as the difference between the set point matrix and the output of soft sensor (i.e., $y[k]$), is regarded as the input of the proportional controller, and the output of the proportional controller, $u[k] = [u_\theta[k], u_\gamma[k]]^T$, is used to correct drifting clock. The progress of obtaining the correction value, $u[k]$, is modelled as

$$u[k] = K\left(\begin{bmatrix} 0 \\ 0 \end{bmatrix} - y[k]\right) = -Ky[k] \tag{15}$$

where $K = \begin{bmatrix} \alpha & 0 \\ 0 & \beta \end{bmatrix}$ is the matrix of proportional controller gain. α and β are the proportional parameters of measured offset and skew respectively.

Therefore, the closed-loop control system of proportional controller can be described by

$$\begin{cases} x[k+1] = A^m x[k] + Bu[k] + G\mu[k] + \omega[k] \\ y[k] = Cx[k] + \nu[k] \\ u[k] = -Ky[k] \end{cases} \tag{16}$$

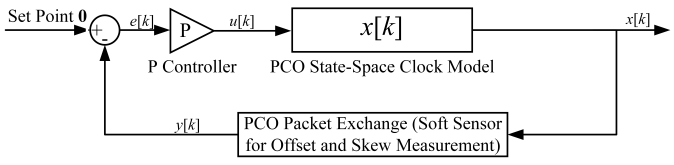

Fig. 2. State Feedback for PCO Clock Synchronization.

where $B = \begin{bmatrix} 1 & 0 \\ 0 & 1 \end{bmatrix}$ denotes PCO clock correction input matrix. To enable the stability of the closed-loop system, the eigenvalue of matrix $(A^m - BKC)$ should be in the unit circle [12]. On the other hand, the proportional controller gain matrix K should be chosen to ensure the module of $(A^m - BKC)$ be not greater than 1. The eigenvalue of closed-loop control system with proportional controller is

$$\lambda_1 = 1 - \alpha, \quad \lambda_2 = 1 - \beta \ (when\ p = 1)$$

The proportional parameter α and β are able to be set to the specified value to enable the closed-loop system of PCO clock state-space model stable or marginally stable (i.e., $\alpha \in (0,1]$ and $\beta \in (0,1]$). The proportional controller can therefore ensure the drifting PCO clock move into steady state. This means that, time synchronization is obtained in the wireless sensor networks.

V. Simulations and Results

As shown in Fig. 1, two kinds of single-hop network topologies, consisting of one master node with *reference clock* and 50 slave nodes with drifting clocks, are simulated to evaluate the performance of pulse-coupled oscillators synchronization in open-source software simulator developed by [16]. Two different drifting PCO clocks are considered in the simulations: the higher performance one (Clock A) with the standard deviation of offset noise and skew noise $\omega_\theta = 10^{-7}$ and $\omega_\gamma = 10^{-9}$ respectively, while the standard deviation of offset noise and skew noise of lower performance oscillator (Clock B) are $\omega_\theta = 10^{-6}$ and $\omega_\gamma = 10^{-8}$ respectively [7]. The threshold of PCO clock state is configured to $1s$ (i.e., time synchronization cycle is also $1s$), and the clock update frequency is $32.768kHz$ to replicate the Real-Time Clock. The *SYNC* packet is set to 21 bytes based on the ZigBee standards [4], [6]. Moreover, the standard deviation of timestamp noise is configured to 10^{-8} to simulate the accurate timestamp [7]. The configurations of simulations are summarized in Table 1.

TABLE I
Simulation Configurations

Symbol	Value	Unit
θ_0	$[10, 15, 20, 25, ..., 100, 105, 110, 120, ..., 200]$	Millisecond
γ_0	$[0, 4, 8, 12, ..., 96, 100]$	PPM
κ	0.48	Millisecond
α	1.0	
β	$[0.5, 1.0]$	

A. Two-Node Network

Fig. 3 indicates that the network consisting of one master and one slave nodes can achieve synchronization from initial offset θ_0. Since the accurate timestamp with standard deviation of $10^{-8}us$ is adopted in the simulation, the high accuracy timestamp and measurement offset are obtained, and the proportional parameters α and β therefore can be

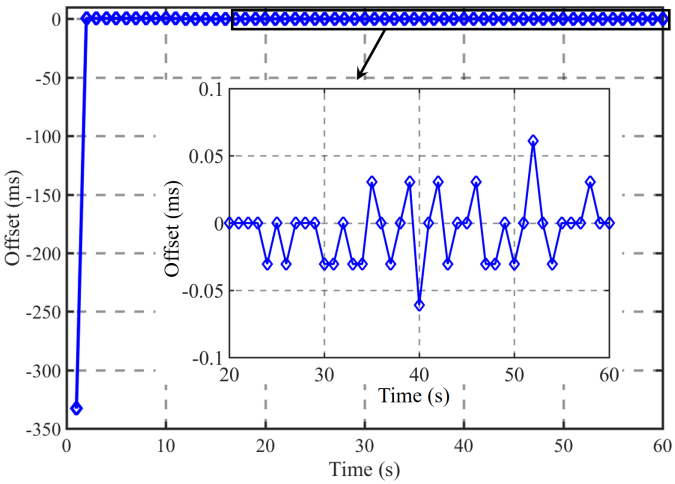

Fig. 3. Offsets of Clock A under the state feedback correction scheme ($\alpha = 1$, $\beta = 0.5$).

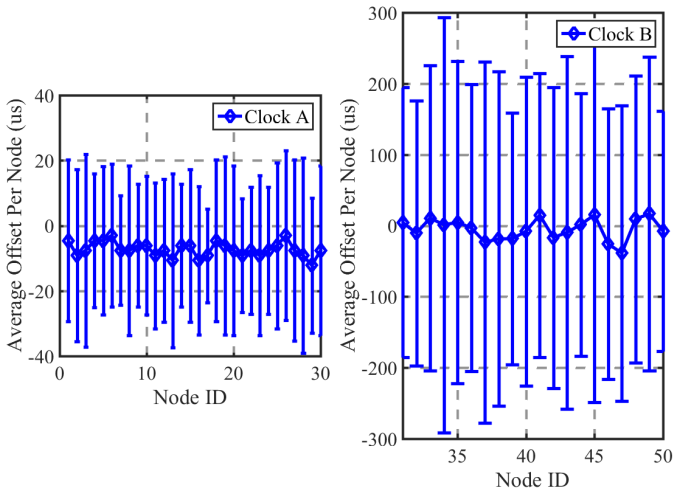

Fig. 4. Average offset of Clock A and Clock B in network topology II ($\alpha = 1$, $\beta = 0.5$).

configured to 1 and 0.5 respectively, the mean and standard deviation of achieved time synchronization precision are $-3.5572 \times 10^{-10} us$ and $24.2529 us$ respectively.

B. Partially-Connected Network

Fig. 4 demonstrates the performance of PCO time synchronization in network topology II. The circle represents the mean of synchronization error with respect to the *reference clock* of master node, and the up bar and low bar are the mean value plus/minus its corresponding standard deviation, representing the variation of the synchronization error for each slave node clock. Since the slave nodes with the ID from 1 to 30 are equipped with higher performance Clock A, and lower performance Clock B is equipped in the slave nodes from 31 to 50. The achieved synchronization of slave nodes with Clock A is obviously more accurate than that of the slave nodes equipped with Clock B.

Even though initial condition (i.e., θ_0 and γ_0) is configured with different value, the slave nodes equipped with the same quality clock can achieve the almost same precision. Specifically, the slave nodes with Clock A can achieve the accuracy with $40us$, and the slave nodes with Clock B can obtain the synchronization accuracy with $300us$. Thus, the initial condition has no effect on the accuracy of PCO synchronization in WSNs. Furthermore, compared with the clock update interval of $30.5us$, the slave nodes with Clock A can achieve time synchronization with precision of $40us$, Clock A is therefore recommended.

C. Fully-Connected Network

Fig. 5 shows the synchronization performance in network topology I. Although the same simulation configurations in topology II are adopted, the achieved accuracy dramatically goes down to $3500us = 3.5ms$ approximately.

Even though [10] simulated the network consisting of 10 non-identical oscillators synchronizes up to certain precision

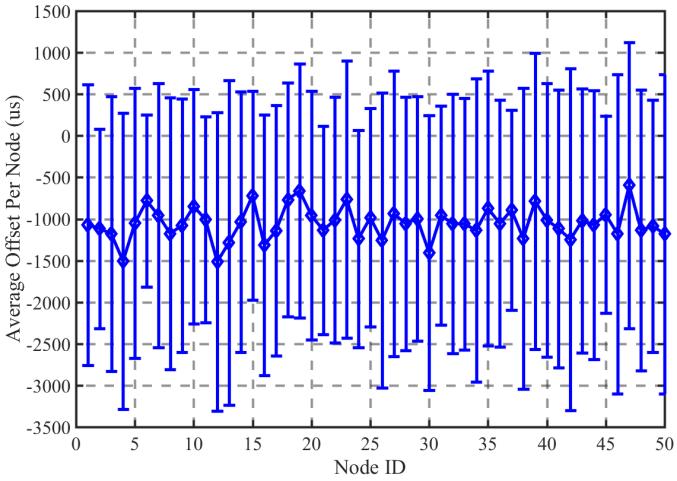

Fig. 5. Average offset of Clock A and Clock B in fully-connected network I ($\alpha = \beta = 1$).

bound $0.051s = 51ms$ by using inhibitory coupling mechanism (Table 3 in [10]), it is clear that the hybrid coupling mechanism can achieve the synchronization with the precision of $3.5ms$ in network topology I.

Conclusion

In this paper, a novel pulse-coupled non-identical oscillators model is proposed to describe a realistic clock oscillator with non-identical and time-varying frequency. A hybrid coupling (i.e., state feedback clock correction) is also introduced to correct the drifting PCO clock. Furthermore, it is shown that a fully-connected wireless sensor network consisting of 50 non-identical and time-varying pulse-coupled oscillators can achieve the synchronization with the precision of $3.5ms$. Similarly, it is demonstrated that a partially-connected wireless sensor network obtains the synchronization with the precision of $40us$ when all sensor nodes in the network are equipped with a specified clock. As a future research work, the pulse-

coupled non-identical oscillators model with non-identical and time-varying frequency will be extended to the multi-hop wireless sensor networks to evaluate its performance.

ACKNOWLEDGMENT

Yan Zong gratefully acknowledges financial support from the University of Northumbria at Newcastle *via* a postgraduate research studentship.

REFERENCES

[1] Z. An, H. Zhu, X. Li [Xinrong], C. Xu, Y. Xu, X. Li [Xiaowei]., Non-identical Linear Pulse-Coupled Oscillators Model with Application to Time Synchronization in Wireless Sensor Networks, IEEE Transactions on Industrial Electronics, vol. 58, issue 6, pp. 2205-2215, Jun 2011.

[2] I. Bojic and M. Kusek., Self-Synchronization of Nonidentical Machines in Machine-to-Machine Systems, in International Conference on Self-Adaptive and Self-Organizing Systems, Philadelphia, USA, 2013, pp. 265-266.

[3] J. A. Boyle, J. S. Reeve, A. S. Weddell., Distinct: Synchronizing Nodes with Imprecise Timers in Distributed Wireless Sensor Networks, IEEE Transactions on Industrial Informatics, vol. 13, issue 3, pp. 938-946, Jun 2017.

[4] F. Eady., Hands-On ZigBee: Implementing 802.15.4 with Microcontrollers, Oxford: Newnes, 2010.

[5] U. Ernst, K. Pawelzik, T. Geisel., Delay-Induced Multistable Synchronization of Biological Oscillators, Physical Review E, vol. 57, issue 2, pp. 2150-2162, Feb 1998.

[6] S. Farahani., ZigBee Wireless Networks and Transceivers, Oxford: Newnes, 2011.

[7] G. Giorgi and C. Narduzzi., Performance Analysis of Kalman-Filter-Based Clock Synchronization in IEEE 1588 Networks, IEEE Transactions on Instrumentation and Measurement, vol. 60, issue 8, pp. 2902-2909, Aug 2011.

[8] B. R. Hamilton, X. Ma, Q. Zhao, J. Xu., ACES: Adaptive Clock Estimation and Synchronization Using Kalman Filtering, in ACM International Conference on Mobile Computing and Networking, San Francisco, USA, 2008, pp 152-162.

[9] Y. Huang, T. Li, X. Dai, H. Wang, Y. Yang., TS2: A Realistic IEEE1588 Time-Synchronization Simulator for Mobile Wireless Sensor Networks, SIMULATION, vol. 91, issue 2, pp. 164-180, Jan 2015.

[10] J. Klinglmayr and C. Bettstetter., Self-Organizing Synchronization with Inhibitory-Coupled Oscillators, ACM Transactions on Autonomous and Adaptive Systems, vol. 7, issue 3, pp. 1-23, Sep 2012.

[11] R. E. Mirollo and S. H. Strogatz., Synchronization of Pulse-Coupled Biological Oscillators, SIAM Journal on Applied Mathematics, vol. 50, issue 6, pp. 1645-1662, 1990.

[12] K. Ogata. Modern Control Engineering, 5th ed. Pearson, 2009.

[13] X. Y. Wang, R. K. Dokania, A. B. Apsel., A Crystal-Less Self-Synchronized Bit-Level Duty-Cycled IR-UWB Transceiver System, IEEE Transactions on Circuits and Systems I: Regular Papers, vol. 60, issue 9, pp. 2488-2501, Sep 2013.

[14] W. Yang, M. Hua, J. Zhang, T. Xia, J. Zou, C. Jiang, M. Wang., Enhanced System Acquisition for NB-IO,. IEEE Access, vol. 5, pp. 13179-13191, Jul 2017.

[15] J. Zhang, M. Wang, M. Hua, W. Yang, and X. You., Robust Synchronization Waveform Design for Massive Low-Power IOT, IEEE Transactions on Wireless Communications, vol. 16, issue 11, pp. 7511-7559, Nov 2017.

[16] Y. Zong, X. Dai, Z. Gao., A Software Simulator of Discrete Pulse-Coupled Oscillators (PCO) Time Synchronization in Wireless Sensor Networks, in International Conference on Automation and Computing, Huddersfield, UK, 2017, pp.1-7.